MAGLAY Process—Electro-Magnetic Controlled Overlay Welding Process with ESW*

Shozaburo NAKANO** Noboru NISHIYAMA**
Toshiharu HIRO** Jun-ichiro TSUBOI**

Surfacing with electro-slag welding process is found superior to that with submerged arc welding process in view of the smaller dilution of base metal and stable welding phenomena even with such a wide electrode as 150 mm.

The formation of under-cutting is found to be in close relations to the flow of molten slag and metal which is driven by the electro-magnetic force induced by the welding current. To counteract this force, two solenoids are equipped adjacent to the edges of the electrode. The Lorentz force based on the interaction between welding current and the electromagnetic field forces molten slag and metal to flow toward the side edges of weld pool. The electro-magnetic control technique can improve flatness of the bead surface at the overlap area adjacent to two weld passes.

Welds deposited on SA 533 B C1.1 steel with type AISI 309 strip electrode fully meet the mechanical and chemical requirements of JIS Z 3221, G 0575, and AEC Regulatory Guide 1.43.

1 Foreword

In order to improve corrosion resistance, stainless steel such as SUS 308 or SUS 347 is used for lining the inside of chemical pressure vessels and nuclear reactor core tubes. In the case of steel plate thickness below 40 mm, from economical standpoint, roll clad and explosive clad processes are mostly employed for lining. When the plate thickness exceeds 50 mm, overlay welding processes are generally used.

The overlay processes currently used include

(1) Strip SAW overlay welding
(2) Multi-electrode MIG overlay welding
(3) Plasma arc overlay welding
(4) Metallizing overlay

Processes (3) and (4) are used for special purpose because of their low efficiency namely: a few kilograms deposition rate an hour. So long as the number of electrodes is increased, the multi-electrode MIG process creates no efficiency problem. Because of its nature, the deposit absorbs a large quantity of nitrogen from the atmosphere, another drawback being a considerable weld penetration. The strip SAW overlay process has a dilution ratio of 15 to 20% and up to 75 mm wide electrodes can be used with relatively good efficiency. Consequently, it is the most popular process today, despite its drawback that defects tend to occur at the overlap of beads.

The evaluation of overlay welding techniques is made from the following standpoints.

(1) The ratio of parent metal dilution is held at low values in order to reduce electrode composition and carbon pickup from parent metal.
(2) Electrode width is made wider to increase efficiency.
(3) Bead smoothness including overlap of beads is raised to reduce repair welding.

By taking these factors into consideration, Kawasaki Steel has developed an overlay welding process called the MAGLAY process. This MAGLAY process utilizes the ESW process that employs Joule's heating of slag instead of arc as a welding heat source. As a result, the weld dilution ratio is decreased to about 10% and the serviceable electrode width is expanded to 150 mm. Furthermore, fused slag and metal flow are controlled through the action of external magnetic field, thus improving bead smoothness. This process provides a considerable improvement over the conventional overlay processes.

* Originally published in *Kawasaki Steel Technical Report*, 12 (1980) 1, pp. 177–188 (in Japanese)
** Research Laboratories

2 ESW Overlay Process

As shown in **Fig. 1**, the ESW overlay process makes use of Joule's heating of a fused slag bath formed just after the electrode. It is necessary to make a stable conduction of electricity through the slag in a shallow molten pool of about 10 mm deep. Cation conduction by adding large quantities of fluorides and electro-conduction through addition of TiO_2 and other semi-conductors can be considered in order to raise the electro-conductivity of slag without generating arcs. Additions of large quantities of TiO_2 will result in deteriorating the detachability of slag, therefore, additions of fluorides are preferable.

The result of investigating the conduction type and electro-conductivity of slag by adding CaF_2 or NaF to flux of the $CaO\text{-}SiO_2\text{-}Al_2O_3$ type is shown in

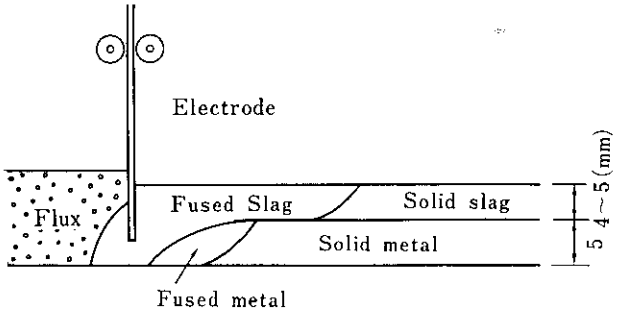

Fig. 1 Schematic view of ESW overlay

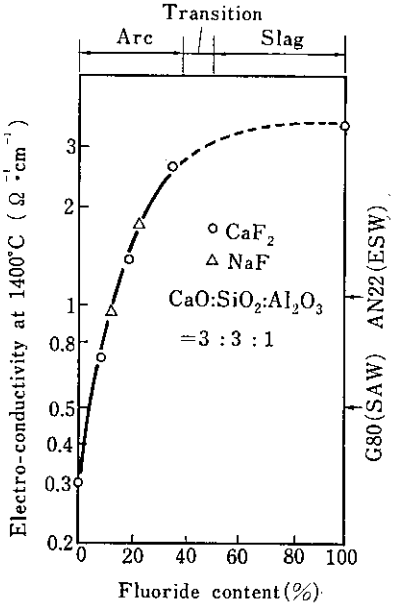

Fig. 2. Effect of fluoride content in flux on electro conductivity and conduction type of welding current

Fig. 2. When the quantity of flourides is less than 40%, it is arc conduction; if it is over 50%, it is slag conduction. The 40 to 50% range is the transition range subject to welding condition. Consequently, additions of fluorides in excess of 50% will be sufficient for performing stable ESW welding. However, to restrict the generation of fluoride type gases due to a reaction, $2CaF_2 + SiO_2 \longrightarrow 2CaO + SiF_4$, additions of CaF_2 are held at slightly less than 50% in flux KFS-150 for the MAGLAY process, and conductivity is maintained by adjusting the remaining composition. Electro-conductivity of KFS-150 is about $3\,\Omega^{-1}\cdot cm^{-1}$, which is much larger than $0.5\,\Omega^{-1}\cdot cm^{-1}$ of ordinary flux for SAW. This is much higher than that of flux AN-22 for ESR and ESW used in the U.S.S.R.

The characteristic of the ESW overlay welding process lies in the mechanism of forming penetration of the parent metal. In other words, in the case of arc fusion, arc is generated from a part of the electrode as shown in **Fig. 3**, and as it moves in the direction of electrode width, penetration is completed. Arc movement is not necessarily uniform: it may be without fusing the parent metal and thus tends to cause incomplete penetration. Since this phenomenon becomes more significant as electrode width becomes wider, the electrode width is limited to 75 mm for practical reason. Also, on the occasion that slag of the preceding pass has not been completely removed from the weld toe, arc is not generated, and it becomes a defect as slag trapped in.

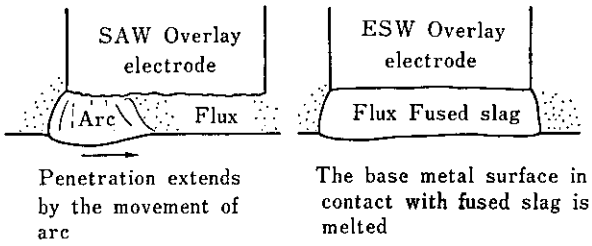

Fig. 3 Penetration characteristics of SAW and ESW overlays

On the other hand, in the case of the ESW overlay welding, the parent metal with which high-temperature slag has come in contact will fuse regardless of the presence of residual slag from the preceding pass, and stable penetration can be obtained. Particularly, in the case of the MAGLAY process, by means of action of the external magnetic field, high-temperature slag in the center of the molten pool is flown toward edges of the molten pool where defects are likely to occur, thus preventing insufficient penetration.

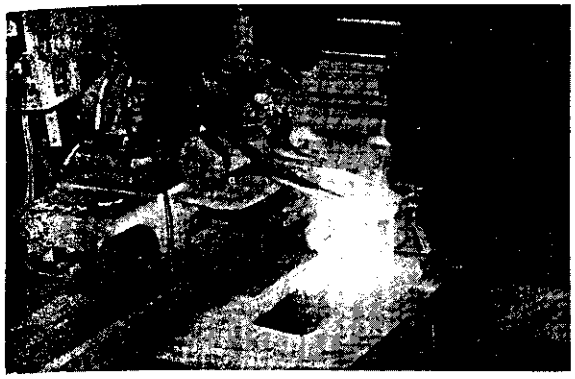

Photo. 1 View of depositing by using 150 mm wide electrode

How overlaying is applied by the MAGLAY process using a 150 mm-wide electrode is shown in **Photo. 1**. In order to prevent overheating from radiation heat of fused slag, the contact jaw is water-cooled. Also, because the shape of a molten pool and the condition of slag flow can be visually inspected, defect-preventive measures can be applied during welding.

3 Prevention of Undercut by the External Magnetic Field

In the ESW overlay welding process, electric current runs in parallel from an electrode to back of the molten pool as shown in **Fig. 4**. Such parallel current has closing effect on slag in conduction and makes the fused slag and fused metals move from edges of the pool toward inside. In consequence, there is a shortage of fused metals at the edges and undercut tends to be generated.

The fluid force F(dyn/cm) created by welding current is as follows.

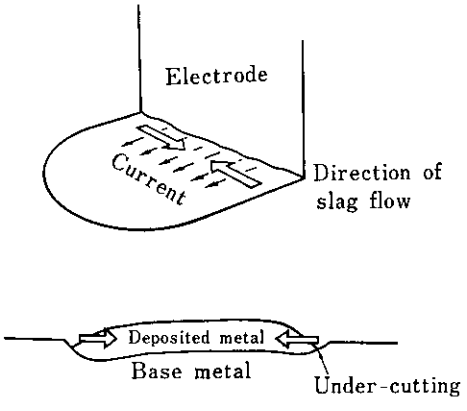

Fig. 4 Schematic mechanism of under-cutting caused by parallel welding current

$$F = iB = i\mu_0 H \quad \cdots\cdots\cdots\cdots\cdots\cdots (1)$$

i: Line density of current (abamp/cm)
B: Magnetic induction (G)
μ_0: Magnetic permeability (H/m)
H: Magnetic field intensity (A/m)

In this case, H is a function of position r from an electrode end to the inside and obtained by equation **(2)**.

$$H(r) = \frac{1}{2\pi}\left(\frac{I}{W}\right)\int_r^{W-r}\frac{dr}{r} = \frac{1}{2\pi}\left(\frac{I}{W}\right)\ln\left(\frac{W-r}{r}\right) \quad \cdots\cdots\cdots (2)$$

I: Welding current (A)
W: Electrode width (cm)

When $W = 15$ cm and $I = 2\,500$ A, an average will be about 700 dyne/cm with a large distribution at the electrode side end.

Undercutting can be prevented by applying externally a fluid force equal to or slightly in excess of this fluid force. Accordingly, in the MAGLAY process, the external magnetic field is utilized to control flow direction and velocity of the fused slag and fused metal. This principle is shown in **Fig. 5**. Lorentz force is generated by the interaction between the external magnetic field perpendicular to the parent metal and welding current, and the force from the center of the molten pool to its edges supplies the fused slag and fused metals to the edges.

Table 1 shows the measured values of magnetic

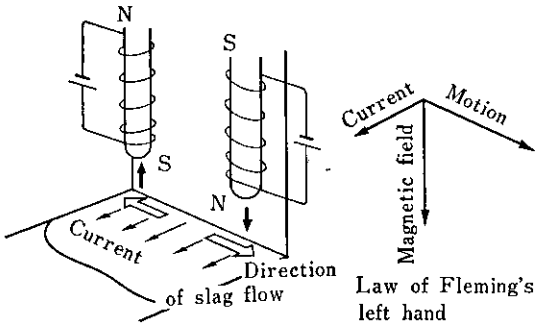

Fig. 5 Control of slag flow with outer magnetic field

Table 1 Relation between current through solenoid coil and electro-magnetic force of Lorentz

Current through solenoid coil*	(A)	1	2	5	10
Magnetic field (measured)	(G)	12.5	42	105	215
Lorentz force (calculated)	(dyn/cm)	200	700	1 743	3 600

* 400 turns

field intensity generated 15 mm below a 400-turn coil and the calculated values of Lorentz force generated by them. A force of 700 dyne/cm is created by a coil current of 2 A, and it is shown that this force can fully meet the fluid force of the fused slag and fused metals by means of a weld current obtained in **Fig. 6**.

How the solenoid coil is attached is shown in **Photo. 2**. In order to avoid radiation heat from the molten pool, the coil is set up in front of the contact jaw and can be controlled left or right independently.

The cross section of a bead obtained is shown in **Photo. 3**.

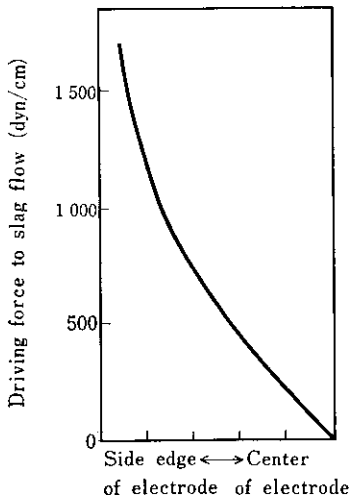

Fig. 6 Calculated driving force to slag flow caused by parallel welding current

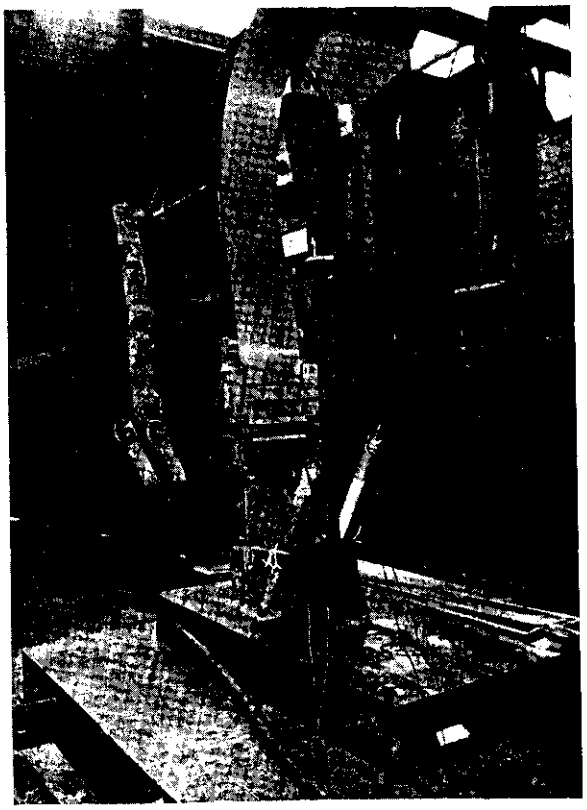

Photo. 2 Feature of MAGLAY welding machine

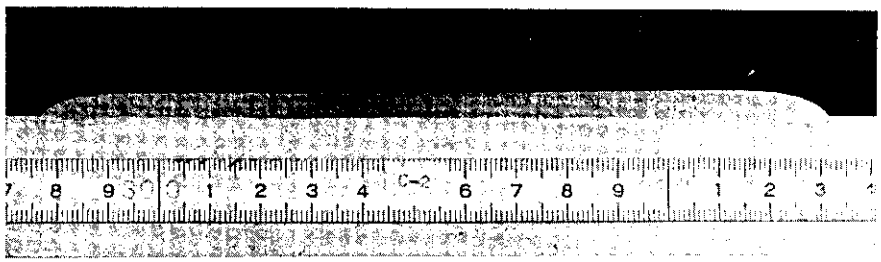

1 pass bead

Location of overlap

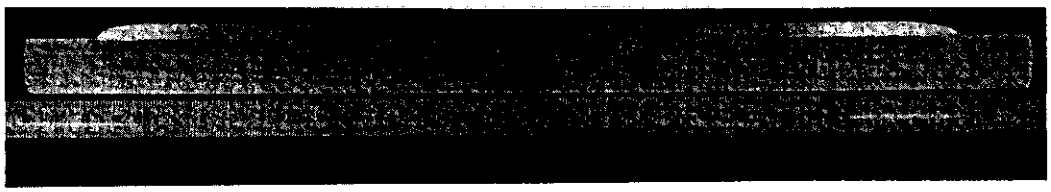

2 passes are laid in parallel

Photo. 3 Examples of transverse section of weld bead

4 Control of Crater Shape by Means of the External Magnetic Field

Crater shape should be used as a criterion for controlling intensity of the external magnetic field. **Photo. 4** presents a relationship between coil current and crater shape. When the magnetic field is not applied, the back edge of crater protrudes at the center considerably, indicating a strong flow from the edge on the side of molten pool to the central part; and a fine continuous undercutting can be observed. At an exciting current of 1 A, welding current is so nonuniformly distributed that the crater is one-sided with a weak magnetic field, and that undercutting is not prevented. At an exciting current of 2 A, the edge in back of the crater has two bulges pointing to the fact that a flow from the center of the electrode to the edge on the side of molten pool was generated, and undercutting can be prevented. Furthermore, as current is increased to 3 A to 5 A, a space between the bulge in the back edge of the crater and concavity becomes wide, suggesting that a flow becomes much faster.

Crater shape when asymmetrical magnetic fields were made to act upon is shown in **Photo. 5**; fused slag makes a turn in one direction and an undercutting on the weak magnetic field side is produced.

Because the dilution ratio tends to increase with a faster slag flow as shown in **Fig. 7**, it is desirable that the external magnetic field is weak so long as an undercutting is not produced. The external magnetic field should be controlled by using crater shape in **Fig. 8** as a criterion.

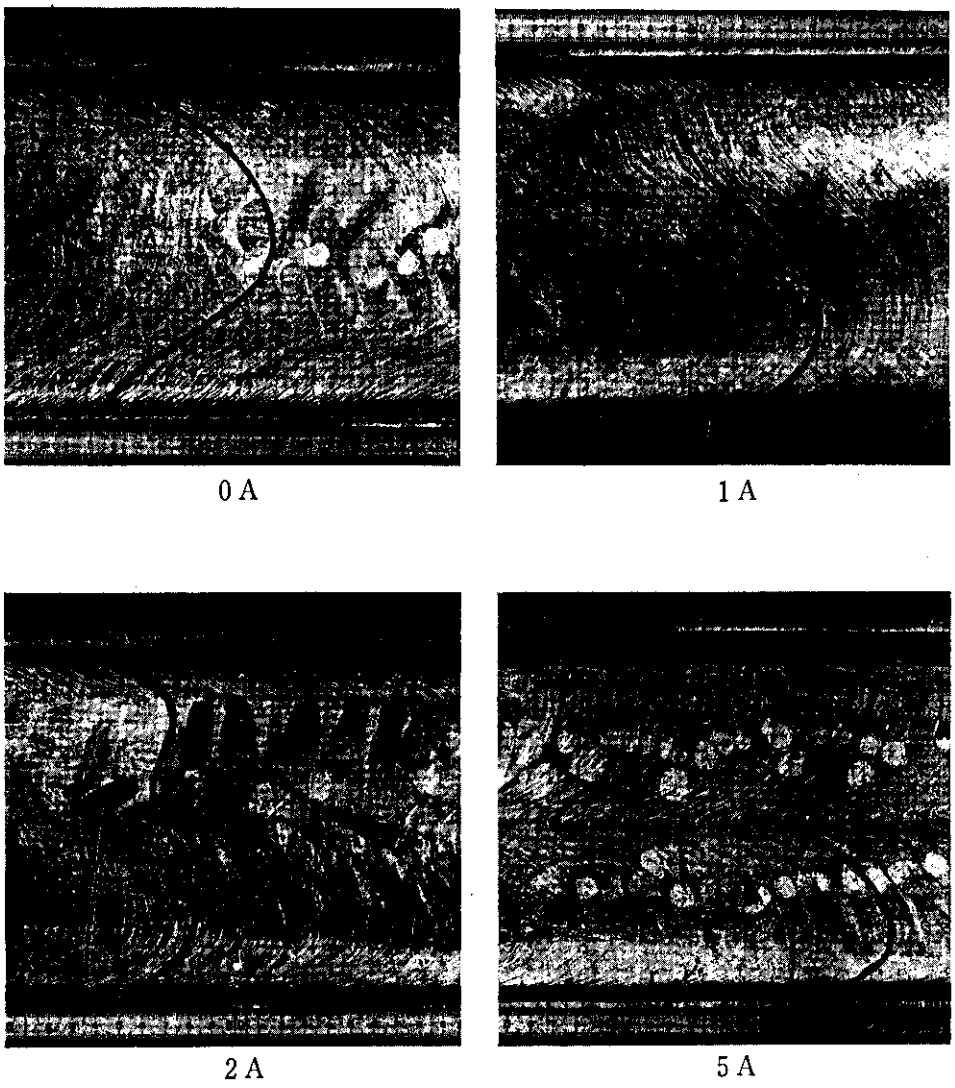

Photo. 4 Effect of magnetic field (exciting current is indicated) on solidification pattern of deposit metal surface

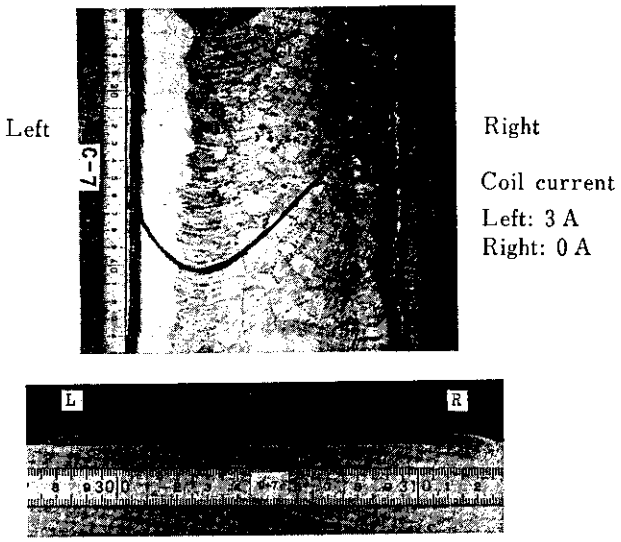

Photo. 5 Irregular solidification pattern of deposit metal surface and under-cutting caused by unbalanced magnetic field

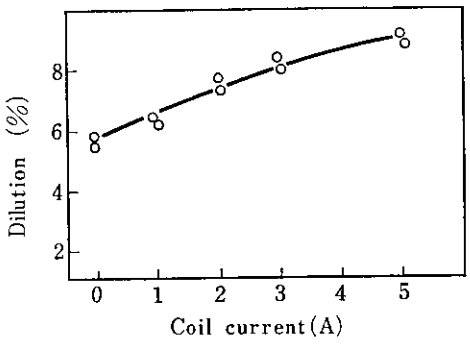

Fig. 7 Effect of magnetic field on dilution of base metal

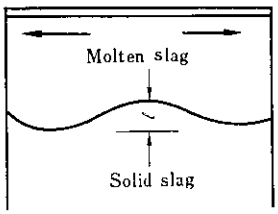

(1) Molten slag should be forced to flow toward the side edges of a weld pool
(2) The distance ℓ must be controlled between 0 to 40 mm.

Fig. 8 Guide to magnetic control of slag flow

5 Changes in Dilution Ratio and Bead Shape Due to Electrode Width

The dilution ratio with constant current density, voltage, and welding speed is presented in **Fig. 9**. Since penetration of bead toe is large in this welding process, the narrower the electrode width the larger the dilution ratio. However, because the dilution ratio varies greatly with welding condition as explained later, it is possible to get a fixed dilution ratio regardless of electrode width so long as proper welding condition is chosen. As shown in **Photo. 6**, cross section of the beads tends to be convex when electrode width becomes narrow. But, in any case, no defects are generated. Note that in the narrow electrodes less than 75 mm wide, current required is small with a small crater. Therefore, it is not necessary to provide a magnetic field in the use of 25, 37.5, and 50 mm wide electrodes.

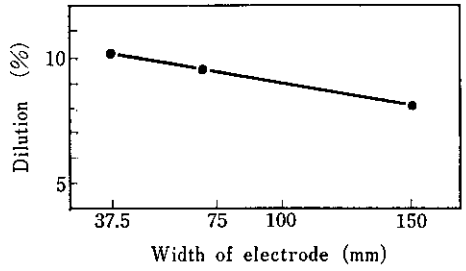

Fig. 9 Influence of electrode width on base metal dilution

6 Deposited Metal Composition

Deposited metal composition $X_{depo}(\%)$ is given by the following equation when electrode composition $X_{elec}(\%)$, parent metal composition $X_{base}(\%)$, dilution ratio α and slag-metal reaction quantity β are used.

$$X_{depo} = (1 - \alpha)X_{elec} + \alpha X_{base} + \beta \quad \cdots\cdots (3)$$

β values obtained from chemical analyses of electrode, parent metal, and deposited metal are shown in **Table 2**. Its characteristics are that as compared with SAW, increment of carbon is small and that oxygen transfer from slag is extremely small. As a result, deposited metals become very clean as shown in **Table 3** and **Photo. 7**.

When slag composition changes, β also changes. For example, by adding Cr_2O_3 to flux, yield of chromium will improve as **Fig. 10** shows.

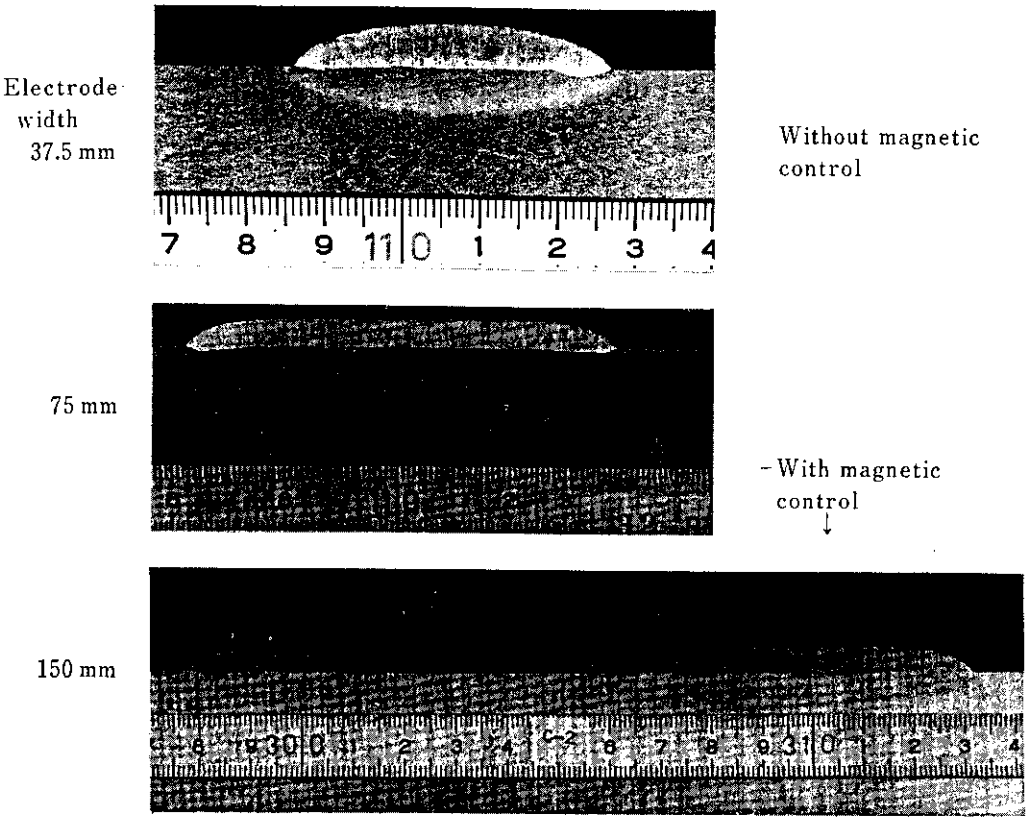

Photo. 6 Transverse section of weld bead deposited with either 37.5, 75 or 150 mm wide electrode

Table 2 Increment, β(%), of chemical contents by slag-metal reaction

	C	Si	Mn	P	S	Ni	Cr	Nb	N	O
ESW overlay	0.005	0.15	−0.5	0.004	0	0	−0.4	−0.2	0	0.01
SAW overlay	0.02	—	—	0.004	0	0	—	−0.2	0	0.06

$X_{depo} = (1-\alpha)\, X_{elec} + \alpha X_{base} + \beta$

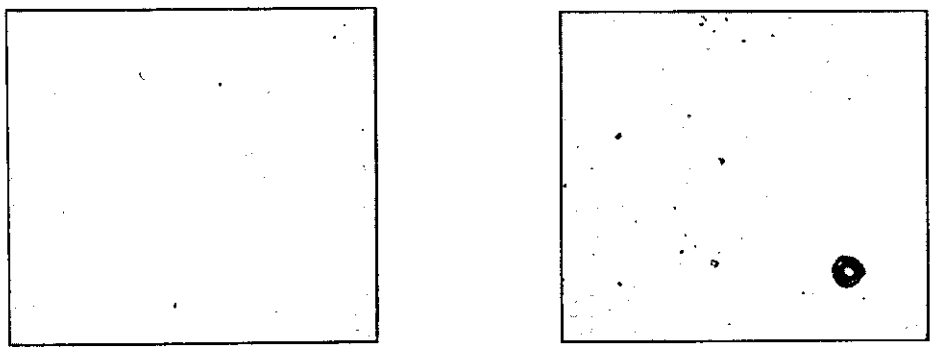

Deposited with MAGLAY (flux: KFS-150) Deposited with SAW (flux: KBS-200)

Photo. 7 Comparison of nonmetallic inclusion content between ESW and SAW overlay deposit metal (× 400)

Table 3 Comparison of cleanliness between ESW and SAW overlay deposit metal

	Oxygen content (%)	Cleanliness*** (%)
SAW overlay *	0.063 7	0.43
ESW overlay **	0.016 7	0.12

* Flux : KBS-200
** Flux : KFS-150
*** Magnification : 3 000

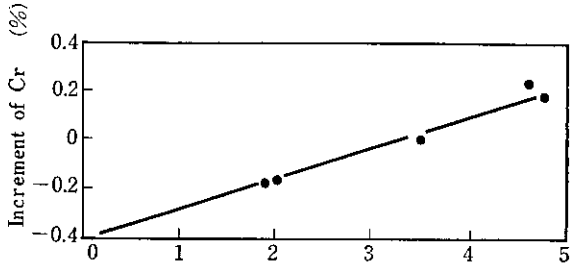

Fig. 10 Influence of Cr_2O_3 content in flux on Cr amount transferred to deposit metal

7 Ferrite Quantity of Deposited Metal

Ferrite quantity of the deposited metal is a critical index to determine high-temperature crack sensitivity, grain boundary corrosion resistance and σ embrittlement sensitivity. In the fablication of chemical plants, 4 to 8% are recommended, while 7 to 15% are recommended for nuclear materials. The relationship between deposited metal composition and ferrite quantity δ(%) can be obtained from De Long's diagram in **Fig. 11**. For the sake of convenience in application, this relationship is mathematically expressed as follows.

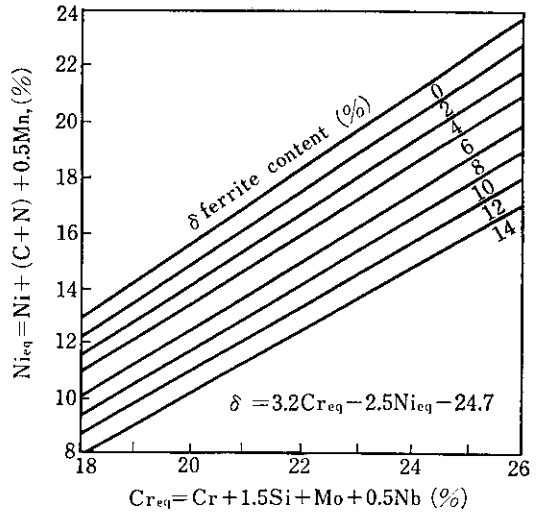

Fig. 11 De Long's diagram

$$\delta_1 = 3.2Cr_{eq} - 2.5Ni_{eq} - 24.7$$
$$= 3.2(Cr_{depo} + Mo_{depo} + 1.5Si_{depo} + 0.5Nb_{depo}) - 2.5\{Ni_{depo} + 30(C_{depo} + N_{depo}) + 0.5Mn_{depo}\} - 24.7 \quad \cdots\cdots (4)$$

When using KFS-150 flux, equation (3) and β in **Table 2** are substituted to obtain equation (5).

$$\delta_2 = (1-\alpha)\{3.2Cr_{elec} + 3.2Mo_{elec} + 1.6Nb_{elec} - 2.5Ni_{elec} + 4.8Si_{elec} - 75(C_{elec} + N_{elec}) - 1.25Mn_{elec}\} + \alpha\{3.2Cr_{base} + 3.2Mo_{base} + 1.6Nb_{base} - 2.5Ni_{base} + 4.8Si_{base} - 75(C_{base} + N_{base}) - 1.25Mn_{base}\} - 25.3 \quad \cdots\cdots (5)$$

When Cr_2O_3 is further added to flux, use of equation (6) will suffice.

$$\delta_3 = \delta_2 + 1.6(\%\, Cr_2O_3) \quad \cdots\cdots (6)$$

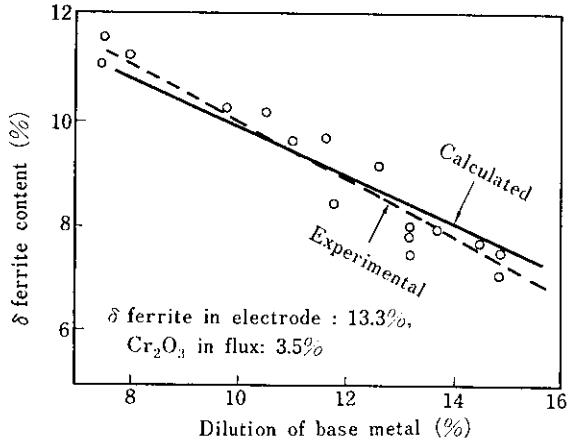

Fig. 12 Comparison between calculated and observed values of ferrite content

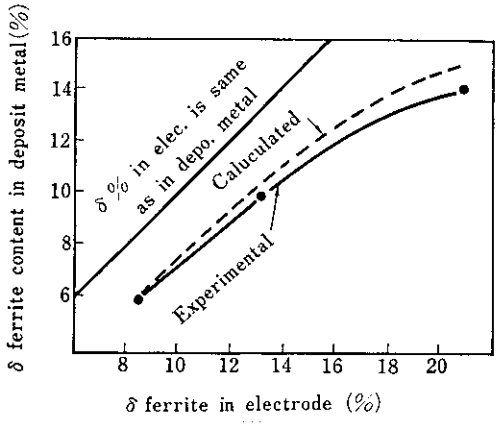

Fig. 13 Comparison of δ ferrite content in deposit metal and that in electrode

An example of experiments using SA 533 steel is shown in **Fig. 12**. At the normal dilution ratio of 8 to 12%, the calculated values are in agreement with measured values by a ferrite scope.

Fig. 13 presents the result of investigating the relationship between ferrite quantities in electrodes and ferrite quantities in deposited metals. Except for the case of an extremely large ferrite quantity in the electrode, calculated values are in agreement with measured values. Moreover, when ferrite quantity in the electrode is within the range of 8 to 15%, it is shown that ferrite quantity in deposited metal is nearly 4% less than that in the electrode.

8 Relationships of Welding Condition with Bead Shape and Ferrite Quantity

The relationships of welding condition with the thickness of reinforcement of weld, dilution ratio, and ferrite quantity are shown in **Figs. 14, 15,** and **16**. Because penetration depth does not alter too much depending on the welding condition, the dilution ratio becomes smaller as the condition becomes such as to enlarge the thickness of reinforcement of weld.

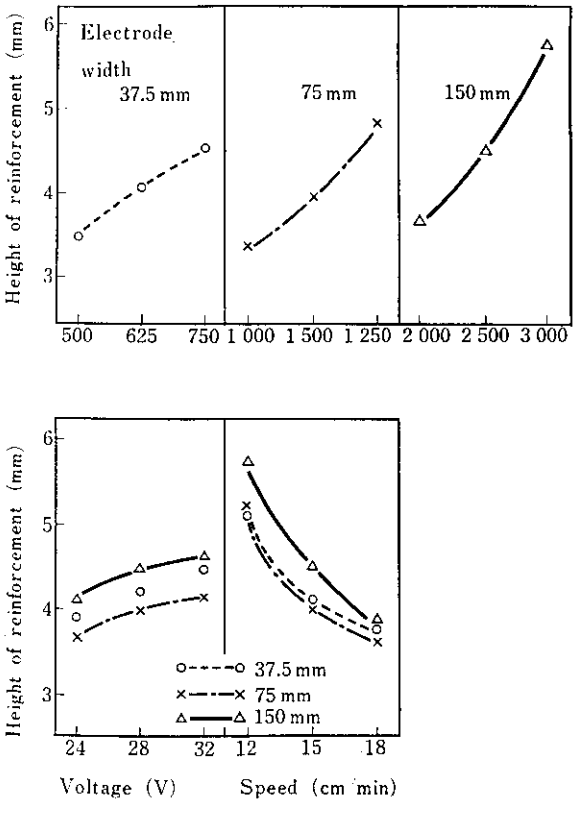

Fig. 14 Effect of welding conditions on height of reinforcement

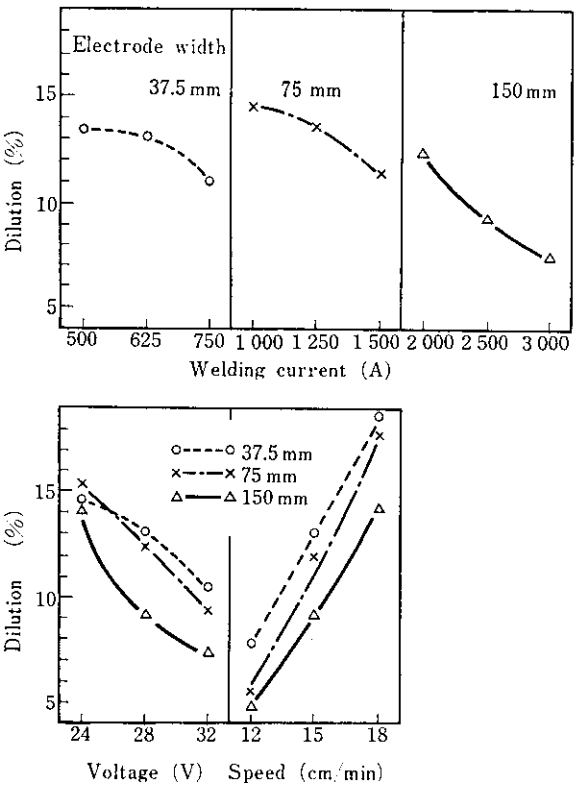

Fig. 15 Effect of welding conditions on dilution of base metal

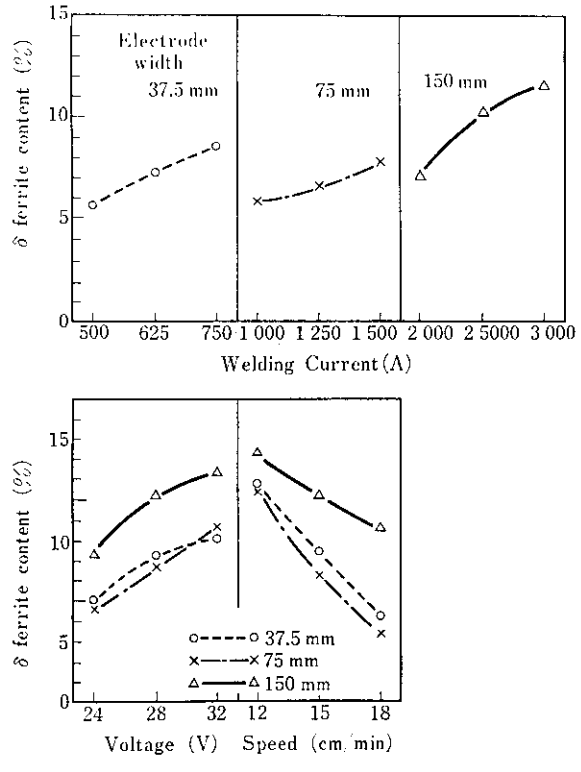

Fig. 16 Effect of welding conditions on δ ferrite content in deposit metal (δ ferrite content in electrode: 13.3%)

Table 4 Base metal used in chemical and mechanical test of MAGLAY deposit metal

Specification	Thickness (mm)	Chemical analysis (%)								
		C	Si	Mn	P	S	Ni	Cr	Mo	V
SA 533 B Cl.1	163	0.18	0.21	1.41	0.006	0.002	0.68	0.09	0.49	0.009

Table 5 Electrode used in chemical and mechanical test

Specification	Size (mm)	Chemical analysis (%)								
		C	Si	Mn	P	S	Ni	Cr	N	δ
KWB-309L	0.4×150	0.021	0.50	2.28	0.019	0.002	11.15	21.35	0.005 5	13.3

9 Mechanical and Chemical Properties of the Deposit

As an example of tests to determine the properties of deposited metal, the results of tests when the type 308 stainless steel is deposited on SA 533 steel are shown below.

The chemistries of the parent metal and electrode are listed in **Tables 4** and **5**, and the welding condition is described in **Table 6**. As shown in **Fig. 17**, beads of three passes were deposited, then, postheating at 615°C was conducted for 45 hours.

As presented in **Table 7** and **Photos. 8** to **11**, the results fully met the specifications.

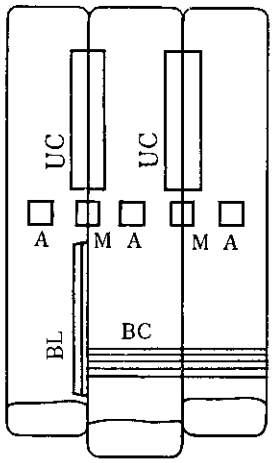

BL: Side bend (L)
BC: Side bend (C)
UC: UCC test
M : Micro stucture and hardness test
A : Chemical analysis

Fig. 17 Sampling location

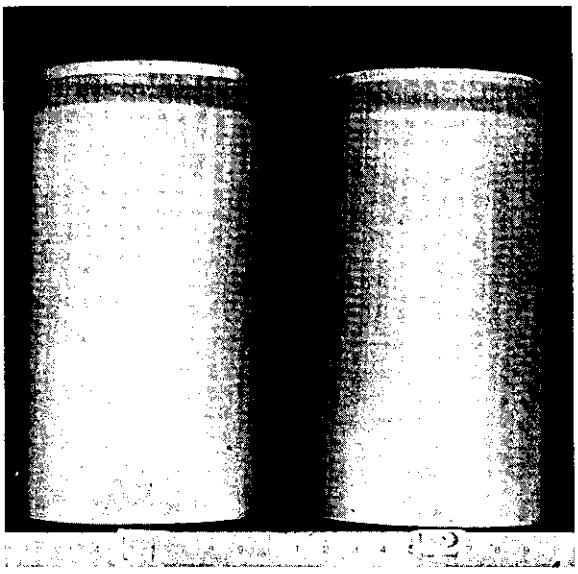

Photo. 8 Results of side bend test (L)

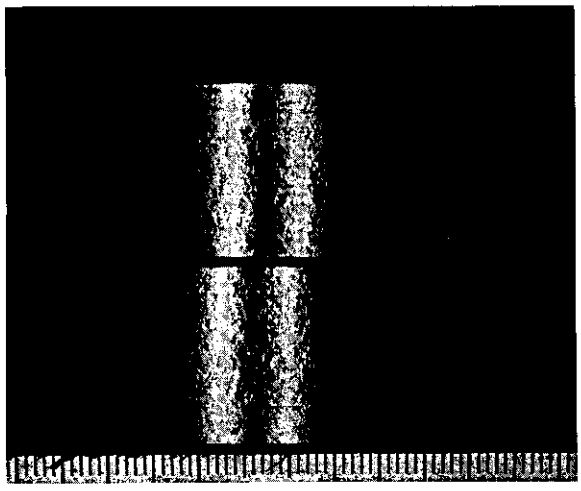

Photo. 9 Corrosion test results conforming to JIS G 0575

Table 6 Welding condition

Current	DCRP 2 500 A	Extension	35 mm
Voltage	28 V	Height of flux	15 mm
Speed	15 cm/min	Post heat	100℃, 10h
Pre-heat	95～200℃		

Table 7 Test results

Item	Result	Specification
Chemical composition of deposit metal (%)	C Si Mn P 0.032 0.33 1.39 0.022 S Ni Cr 0.002 10.07 18.73	JIS Z 3221 C Si Mn P S Nj Cr ≦0.04 ≦0.9 ≦2.5 ≦0.04 ≦0.03 9～12 18～21
Ferrite content	As weld : 9.0～10.2 After SR : 5.7～6.5	≧5, after SR
Side bend	L : No crack C : No creck (cf.Photo.8)	No creck, no inclusion after bending
Corrosion test	No crack (cf.Photo.9)	JIS G 0575, No creck after bending
UCC test	No crack (cf.Photos.10, 11)	AEC Regulatory Guide 1.43 No crack after removing deposit metal

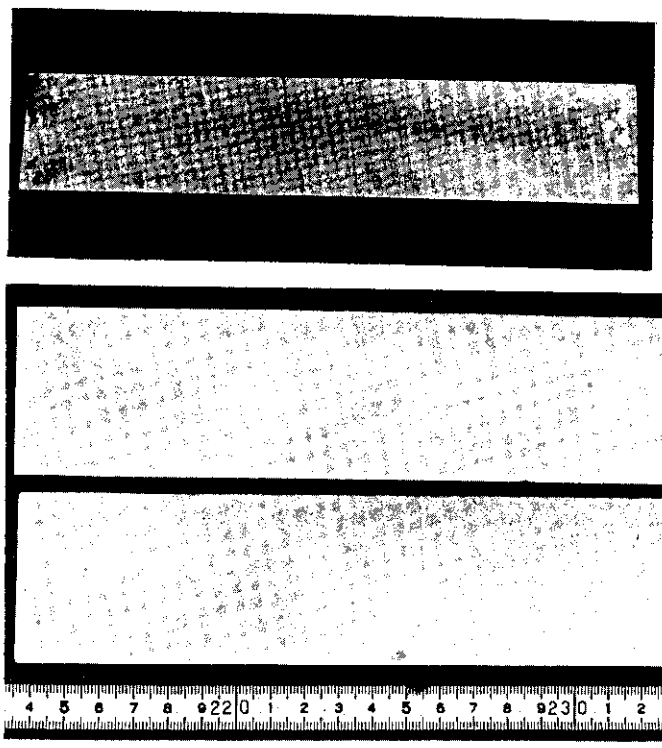

After removal of cladding

Die penetration test

Photo. 10 Results of UCC test

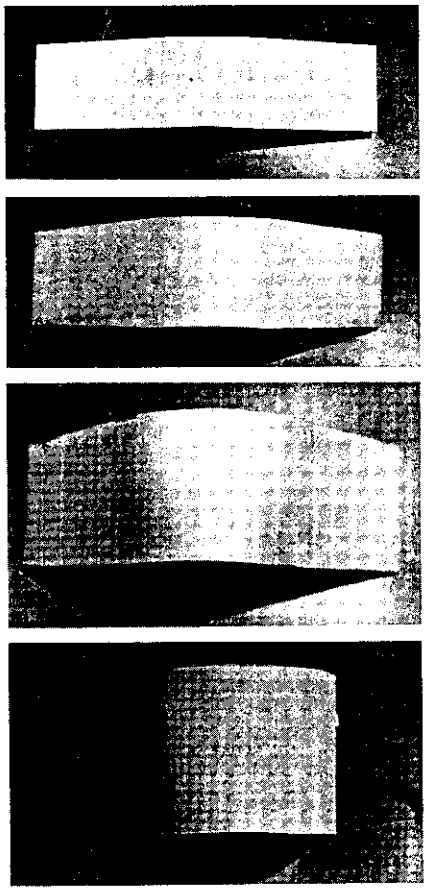

Photo. 11 Results of UCC test after bending (G. L.: 50 mm)

10 Conclusion

The MAGLAY process has been developed as a high-efficiency and high-quality overlaying process. In this process, a newly developed flux of special composition is used. By converting the heat source from arc to Joule's heat of slag, the dilution ratio is reduced by about 10%. And serviceable electrode width can be enlarged to 150 mm. Furthermore, by means of action of an external magnetic field, a flow of fused slag and fused metals is controlled, resulting in a very smooth overlay surface including lap bead. Also, when flux KFS-150 developed for the MAGLAY process is used, δ ferrite quantity of deposited metal becomes about 4% less than that in electrode and oxygen in deposited metal drops to 160 ppm as compared with about 600 ppm of the SAW process.

Welds deposited on SA 533 B Cl.1 steel with type 309 strip electrode fully meet the mechanical and chemical requirements of JIS Z 3221, G 0575, and AEC Regulatory Guide 1.43.